Interference of corner reflected and edge diffracted signals for a surface-breaking crack

J. D. Achenbach and A. N. Norris

The Technological Institute, Northwestern University, Evanston, Illinois 60201 (Received 10 November 1980; accepted for publication 27 January 1981)

Backscatter of time-harmonic longitudinal waves from a surface-breaking crack is investigated in the high-frequency range. It is assumed that the distance of the transducer to the crack is large as compared to the crack depth, and that the incident rays are normal to the crack edge. The crack length is assumed much greater than its depth. A two-dimensional model for the transducer is considered. In the time domain, the first and second received signals are the edge-diffracted signal and the corner-reflected signal, respectively. These signals are analyzed in the frequency domain, by using the uniform asymptotic theory of diffraction. The response of the transducer due to the interference of the two signals is calculated. It is shown that the transducer's response is a sensitive function of its position.

PACS numbers: 43.20.Fn, 43.20.Bi, 43.20.Dk

INTRODUCTION

In the geometry shown in Fig. 1 a transducer is positioned relative to a surface-breaking crack such that the emitted signal is reflected to the transducer by the corner at the crack mouth. In the time domain the corner reflection is, however, preceded by another distinct signal which is due to diffraction from the crack edge. As the transducer is moved slightly, the relative amplitudes of the two signals may change dramatically. This will happen when the transducer is located at the boundary of the zone of reflected waves.

The interference between these two signals, which can be most graphically displayed in the frequency domain, provides essential information for the determination of the crack depth. The most distinct interference is obtained when the two signals are of the same order of magnitude.

For high-frequency (short) pulses, ray theory provides a very useful method to analyze interference phenomena in the frequency domain. In an elastic solid there are rays of longitudinal motion (L rays) and rays of transverse motion (T rays). Unfortunately, it is rather complicated to analyze fields at shadow boundaries and at boundaries of zones of reflected waves. The simplest high-frequency theories, i.e., geometrical elastodynamics (GE) and geometrical theory of diffraction (GTD) are not valid near such boundaries. In this paper we estimate the relative amplitude of the edge diffraction and the corner reflection by using uniform asymptotic theory, which provides corrections to GE and GTD at shadow boundaries and boundaries of zones of reflected waves.

The results that are presented here are valid at high frequencies, in the farfield, and for a two-dimensional approximation. By high frequency we mean that $k_L d \gg 1$ (where $k_L = \omega/c_L$ and d is the crack depth), and by farfield that $d/r \ll 1$, where r is the distance from transducer to crack mouth. For a two-dimensional configuration we assume a line source behavior for the transducer. Implicit in this two-dimensional model is that the crack width is much larger than the transducer width.

The use of ultrasonic methods to *detect* internal as well as surface defects is now well established. In recent years these methods have been refined to determine the *size*, *shape*, and *orientation* of cracks. For a review of both bulk and surface wave ultrasonic methods for the measurement of the depth of surface-breaking cracks we refer to a paper by Doyle and Scala. A recent paper by Golan *et al.*, describes current work on ultrasonic diffraction techniques for the characterization of fatigue cracks.

It is assumed that the faces of the crack do not interact with each other. Thus the crack never completely closes. This is a realistic assumption if the crack is actually a thin slit of finite width, or if a static prestress has been applied. If the crack faces would interact, corner reflection and edge diffraction would still occur, but these effects would be weaker.

I. RAY GEOMETRY

We consider a surface-breaking crack of depth d normal to the free surface I, at a distance b from a vertex of interior angle ϕ , $0 < \phi < \pi/2$. The transducer is free to be shifted along the free surface II. A position of the transducer is defined by x, where x is the distance of the center of the transducer from Q, the intersection

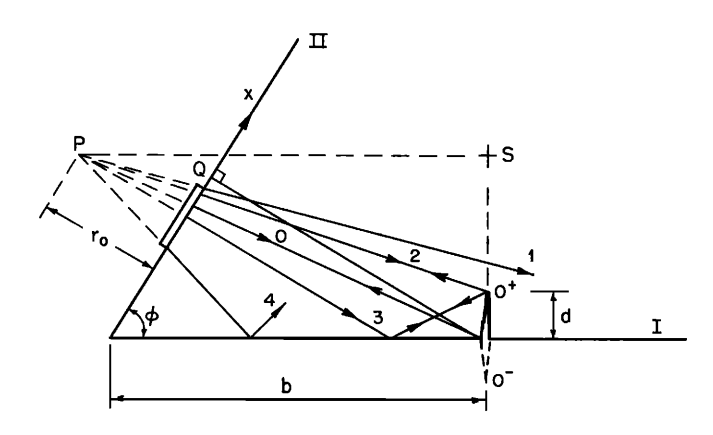


FIG. 1. Ray geometry of transducer and surface-breaking crack.

165

of II and the normal to II from the crack mouth. The distance x is defined as positive in the direction away from the vertex, so, for example, in Fig. 1: x < 0. We define the distance $r = b \sin \phi$ as the distance from Q to the crack mouth.

Some insight in the geometry of the boundaries of zones of reflected waves can easily be obtained on the basis of simple geometrical ray-theory considerations. Let us assume that the transducer emits a beam of L rays (longitudinal waves) of vertex angle $2\psi_0$, The rays appear to emanate from a virtual source P, as shown in Fig. 1. Each ray of the beam is defined by an angle ψ , where $\psi \epsilon (-\psi_0, \psi_0)$, and ψ is measured clockwise from the central ray.

Part of the beam emitted by the transducer will impinge upon the crack. In Fig. 1 the rays 1 and 4 do not interact with the crack. Ray 2 is diffracted by the crack edge to produce a cylindrical wave emanating from the crack edge. The beam between rays 2 and 0 is first reflected by the crack and then reflected from surface 1. Conversely the beam between rays 0 and 3 is first reflected by I and then reflected by the crack. Together the crack and surface I generate a "reflection" which is directed back towards the transducer and which is referred to as the corner reflection. The corner reflection is detected by the transducer as a signal with a different phase and amplitude than the edge-diffracted signal.

In addition to corner reflection and edge diffraction one might consider diffraction at the point where the crack intersects the free surface (the crack mouth). For wedges of vertex angle $\leq \pi$, this diffraction is, however, thought to be negligible.

For the present purpose we are interested only in the field in a direction close to the direction of the incident rays. Let us consider an L ray with a signal of initial amplitude $A(\psi)$, incident at an angle $(\pi/2 - \phi + \psi)$ on the free surface I. For simplicity we assume that the incident wavefront is essentially plane. After reflection the amplitude on the reflected L ray then is $R_L^L(\pi/2 - \phi + \psi)A(\psi)$, where the reflection coefficient $R_L^L(\theta_L)$ is defined by

$$R_L^L(\theta) = \frac{\sin 2\theta_L \sin 2\theta_T - \kappa^2 \cos^2 2\theta_T}{\sin 2\theta_L \sin 2\theta_T + \kappa^2 \cos^2 2\theta_T}.$$
 (1)

Here

166

$$\kappa = c_L / c_T, \tag{2}$$

where $c_L = [(\lambda + 2\mu)/\rho]^{1/2}$ and $c_T = (\mu/\rho)^{1/2}$ are the velocities of longitudinal and transverse waves, respectively, and θ_T is defined by Snell's law.

$$\cos\theta_T = \kappa^{-1} \cos\theta_L \,. \tag{3}$$

The rays reflected from I are next reflected by the crack, and they produce a reflection boundary in the direction of the incident ray. An incident L ray also generates mode-converted T rays at surface I. These T rays are incident upon the crack at an angle less than the critical angle, and so do not generate reflected L

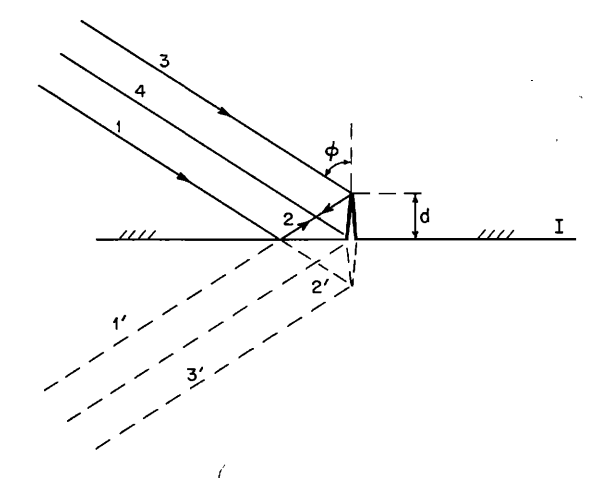


FIG. 2. Image beam for corner reflection.

rays. The same T rays do generate diffracted L rays at the crack edge. However, these cylindrically diffracted L rays are of negligible magnitude as compared with the corner reflected L-L-L rays. This will be more evident once we have calculated the corner reflection magnitude. Hence for the present purpose only the L-L-L rays need be considered for reflection of L rays first from I and then from the crack surface. It can be verified that the same statements can be made for rays which are first reflected from the crack, and then from surface I.

Thus, for the field near the transducer, we only need to consider L-L-L reflections. With this in mind we may view the reflection problem in terms of an image source which generates rays carrying waves of amplitude $R_L^L(\pi/2-\phi+\psi)A(\psi)$ incident upon a crack of length 2d in an unbounded medium. This change of amplitude and source direction is equivalent to including the reflections at I implicitly, but excluding mode conversions. The geometry is shown in Fig. 2. In Fig. 2 the ray path $L_3L_2L_1$ for the original beam becomes the path $L_3'L_2'L_1$, for the image beam; $L_1L_2L_3$ becomes $L_1'L_2L_3$, etc.

With respect to the incident image beam and the crack in an unbounded solid the simple geometrical ray-theory considerations must now be extended to obtain an accurate representation of the scattered field near the reflection boundary of the L rays. This can be done by uniform asymptotic theory as discussed in the next section.

II. 2-D SCATTERING OF A PLANE LONGITUDINAL WAVE BY A CRACK

As a preliminary to the analysis of scattering by a surface-breaking crack we investigate the scattering of a plane longitudinal wave by an interior crack. A crack of uniform width 2d is shown in Fig. 3. The x_3 axis is parallel to the edges of the crack, and the crack is defined by $x_2 = 0$, $|x_1| \le d$. An incident plane longitudinal wave is defined by

$$\mathbf{u}^{i} = A\mathbf{p} \exp(ik_{L}\mathbf{p} \cdot \mathbf{x}), \tag{4}$$

where

J. Acoust. Soc. Am., Vol. 70, No. 1, July 1981

J. D. Achenbach and A. N. Norris: Diffracted signals for a crack

$$\mathbf{p} = (\cos \theta_L, \sin \theta_L, 0). \tag{5}$$

Since both the incident wave and the scattering obstacle are independent of the x_3 coordinate, the scattering problem is two-dimensional in character.

A. Geometrical elastodynamics (GE)

We will first consider the geometrical elastodynamics field. In GE the incident wave and the geometrical reflection from the illuminated face of the crack are taken into account. For an unbounded plane of reflection the reflected wave is

$$\mathbf{u}^{r} = \sum_{\beta=L, T} \mathbf{u}^{\beta}, \tag{6}$$

where

$$\mathbf{u}^{\beta} = AR_{\beta}^{L}(\theta_{L})\mathbf{d}^{\beta}\exp(ik_{\beta}\mathbf{p}^{\beta}\cdot\mathbf{x}). \tag{7}$$

In Eq. (7), $R_{\beta}^{L}(\theta_{L})$ is the reflection coefficient for reflection of an incident longitudinal wave as a wave of type β ($\beta = L$ or $\beta = T$). Also

$$\mathbf{p}^{\beta} = (\cos\theta_{\beta}, -\sin\theta_{\beta}, 0), \tag{8}$$

where θ_T satisfies Snell's law given by Eq. (3), and

$$\mathbf{d}^{L} = \mathbf{p}^{L}, \quad d^{T} = (\sin \theta_{T}, \cos \theta_{T}, 0). \tag{9}$$

Quantities associated with the crack edges at $x_1 = -d$ and $x_1 = +d$ are labeled by 1 and 2, respectively. In accordance with Eq. (6) the GE field can then be written as

$$\mathbf{u}^{ee} = [H(t_1) + H(t_2) - H(-x_2)]\mathbf{u}^{i}$$

$$+ \sum_{\beta=L, T} [H(s_{\beta 1}) + H(s_{\beta 2}) - H(-x_2)] \mathbf{u}^{\beta}.$$
 (10)

Here $H(\cdot)$ is the Heaviside step function, and $t_{\it j}$ and $s_{\it kj}$ are defined as

$$t_i = (2k_L R_i)^{1/2} \sin \frac{1}{2} (\theta_i - \theta_{L_i}), \qquad (11)$$

$$s_{\theta,i} = -(2k_{\theta}R_{i})^{1/2}\sin\frac{1}{2}(\theta_{i} + \theta_{\theta,i}),$$
 (12)

where

167

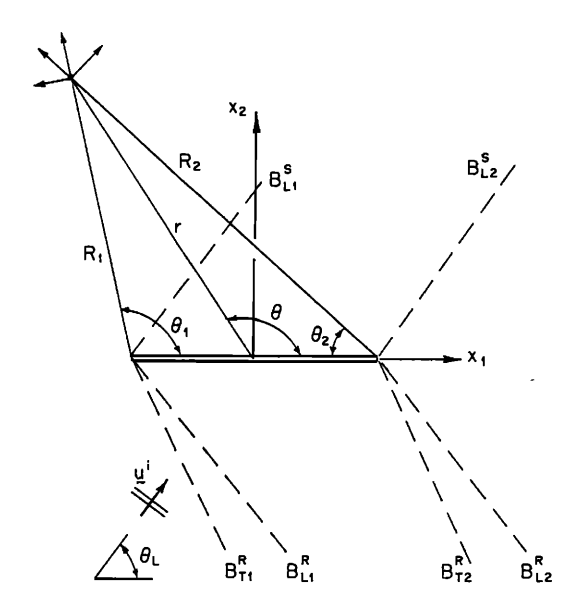


FIG. 3. 2-D scattering by a crack.

$$\theta_{\beta_1} = \theta_{\beta_1}, \quad \theta_{\beta_2} = \pi - \theta_{\beta_1}, \quad \beta = L, T,$$
 (13)

and θ_L and θ_T are related by Snell's law (3). The angles θ_1 and θ_2 are defined in Fig. 3. Equation (10) shows that the GE field is discontinuous at the shadow boundaries B_{L1}^S and B_{L2}^S , and at the boundaries of the geometrically reflected field, $B_{\beta_f}^R$. These boundaries are also shown in Fig. 3.

B. Geometrical theory of diffraction (GTD)

Within the context of GTD, the field carried by the primary diffracted body-wave rays are

$$\begin{split} \mathbf{u}_{\beta}^{L} &= A(k_{\beta}R_{1})^{-1/2}D_{\beta}^{L}(\theta_{1};\theta_{L1})\exp[i(k_{\beta}R_{1} - k_{L}p_{1}d)\mathrm{d}^{\beta_{1}} \\ &+ A(k_{\beta}R_{2})^{-1/2}D_{\beta}^{L}(\theta_{2};\theta_{L2})\exp[i(k_{\beta}R_{2} + k_{L}p_{1}d)]\mathrm{d}^{\beta_{2}}, \end{split} \tag{14}$$

where $\beta = L$ or $\beta = T$. The angles θ_1 and θ_2 , as well as the distances along the rays, R_1 and R_2 , are shown in Fig. 3. The unit vectors \mathbf{d}^{θ_j} are

$$d^{\beta j} = \begin{cases} [(-1)^{j+1} \cos \theta_j, \sin \theta_j, 0], & \beta = L; \quad j = 1, 2, \\ [(-1)^{j} \sin \theta_j, \cos \theta_j, 0], & \beta = T; \quad j = 1, 2. \end{cases}$$
 (15)

In terms of the polar coordinates r and θ , R_j and θ_j may be expressed as

$$R_{\bullet} = [d^2 + r^2 - 2(-1)^j dr \cos\theta]^{1/2}, \qquad (16)$$

$$\sin\theta_i = (r/R_i)\sin\theta \ . \tag{17}$$

Expressions for the two-dimensional diffraction coefficients $D^L_{\beta}(\theta;\theta_L)$ follow from Ref. 3. In the sequel we will only consider the contribution from the primary diffracted longitudinal wave. The relevant diffraction coefficient is

$$D_L^L(\theta;\theta_L) = \frac{e^{i\tau/4}}{2(2\pi)^{1/2}(\kappa^2 - 1)} \frac{f_1(\theta) + f_2(\theta)}{f_2(\theta)}, \qquad (18)$$

where

$$f_1(\theta) = (\kappa^2 - 2\cos^2\theta)(\kappa^2 - 2\cos^2\theta_L)$$

$$\times (1 - \cos\theta)^{1/2} (1 + \cos\theta_L)^{1/2}, \qquad (19a)$$

$$f_2(\theta) = \sin 2\theta \sin 2\theta_r (\kappa - \cos \theta)^{1/2} (\kappa + \cos \theta_r)^{1/2}, \qquad (19b)$$

$$f_3(\theta) = (\cos\theta - \cos\theta_L)(\kappa_R - \cos\theta)$$

$$\times (\kappa_R + \cos \theta_L) K^+(-\cos \theta) K^+(\cos \theta_L) . \tag{19c}$$

In these expressions

$$\kappa = c_L/c_T, \quad \kappa_R = c_L/c_R \,, \tag{20}$$

$$K^{+}(\zeta) = \exp\left[-\frac{1}{\pi} \int_{1}^{\kappa} \tan^{-1}\left(\frac{4s^{2}(s^{2}-1)^{1/2}(\kappa^{2}-s^{2})^{1/2}}{(\kappa^{2}-2s^{2})^{2}}\right) \frac{ds}{s+\zeta}\right].$$
(21)

It can be shown that $D_L^L(\theta;\theta_L)$ becomes unbounded at the shadow boundary $(\theta=\theta_L)$ and at the boundary of the zones of reflected L waves $(\theta=2\pi-\theta_L)$. For $|\epsilon|\ll 1$

$$\theta = \theta_L - \epsilon, \quad D_L^L(\theta; \theta_L) = \frac{e^{i\tau/4}}{(2\pi)^{1/2}} \frac{1}{\epsilon} + O(1),$$
 (22)

$$\theta = 2\pi - \theta_L - \epsilon, \quad D_L^L(\theta; \theta_L) = \frac{e^{i\pi/4}}{(2\pi)^{1/2}} \frac{1}{\epsilon} R_L^L(\theta_L) + O(1),$$

(23)

J. Acoust. Soc. Am., Vol. 70, No. 1, July 1981

J. D. Achenbach and A. N. Norris: Diffracted signals for a crack

where $R_L^L(\theta_L)$ is defined in (1).

The total field according to GTD is

$$u^{t} = u^{ge} + \sum_{\beta = L, T} u^{L}_{\beta} + O[(k_{\beta} \gamma)^{-1}],$$
 (24)

where u^{ge} and u^{L}_{g} are given by (10) and (14), respectively.

C. Uniform asymptotic theory (UAT)

The GE field, \mathbf{u}^{ge} , is discontinuous across the boundaries B_{Lj}^S and $B_{\beta j}^R$, and the edge-diffracted field, \mathbf{u}_{β}^L , blows up at these boundaries. Appropriate corrections to (24) have been discussed by Achenbach *et al.*³ The correction produces a result which is equivalent to the uniform asymptotic theory (UAT) which has been worked out for acoustics and for electromagnetic theory, see Refs. 4 and 5.

The total field according to UAT is given by

$$\mathbf{u}^{t} = \mathbf{u}^{G} + \sum_{\beta = L, T} \mathbf{u}_{\beta}^{L} + O[(k_{\beta} \gamma)^{-1}], \qquad (25)$$

where \mathbf{u}^G is the following modification of \mathbf{u}^{ge} :

$$\mathbf{u}^{G} = [F(t_{1}) + F(t_{2}) - H(-x_{2})]\mathbf{u}^{i}$$

$$+ \sum_{\beta=L,T} \left[F(s_{\beta_1}) + F(s_{\beta_2}) - H(-x_2) \right] u^{\beta}. \tag{26}$$

Here t_j and s_{β_j} are given by (11) and (12), and

$$F(z) = \frac{1}{\sqrt{\pi}} \int_{-z}^{\infty} e^{i(t^2 - \tau/4)} dt + \frac{1}{2\sqrt{\pi}} \frac{1}{z} e^{i(z^2 + \tau/4)}.$$
 (27)

The function F(z) has the following asymptotic behavior

$$F(z) = H(z) + O(z^{-3}), |z| \to \infty,$$
 (28)

and

$$F(z) = \frac{1}{2\sqrt{\pi}} \frac{1}{z} e^{i\pi/4} + \frac{1}{2} + \frac{z}{2\sqrt{\pi}} e^{-i\pi/4} + O(z^3), \quad |z| \to 0.$$
(29)

It follows from (29) that F(z), and thus \mathbf{u}^G becomes singular at the boundaries of the shadow zone $(\theta_j = \theta_{L_f})$ and the zones of reflected waves $(\theta_j = 2\pi - \theta_{B_f})$. It can, however, be verified that these singularities are exactly canceled by similar singularities in \mathbf{u}_B^L , and thus the total field remains bounded, see (14), (22), and (23) for $\beta = L$. Away from these boundaries t_f and s_{B_f} are large, because $(k_L R_f)^{1/2} \gg 1$, hence (28) applies and we find $\mathbf{u}^G + \mathbf{u}^{fe}$. Thus at $B_{L_f}^S$ and $B_{B_f}^R$ the field is continuous, and away from these boundaries the total field according to UAT reduces to that of GTD.

III. CORNER REFLECTION

We now return to the surface-breaking crack, to consider the application of uniform asymptotic theory. The part of the beam which produces a corner reflection consists of rays defined by the angle ψ , where $\psi \epsilon (\psi_1, \psi_2)$, and ψ_1 and ψ_2 follow from Fig. 1 as

$$\psi_1 = \max(-\psi_0, \psi^-), \quad \psi_2 = \min(\psi_0, \psi^+),$$
 (30)

where

$$\tan(\phi - \psi^{\pm}) = \overline{SP}/\overline{SO}^{\mp} = \frac{(r + r_0)\sin\phi - x\cos\phi}{\pm d + (r + r_0)\cos\phi + x\sin\phi}.$$
(31)

A necessary and sufficient condition for the reflected signal to exist is that $\psi_2 > \psi_1$.

As discussed above the corner reflection of longitudinal waves is equivalent to determining the reflection by an interior crack of an image beam of amplitude $R_L^L(\pi/2-\phi+\psi)A(\psi)$. It is now assumed that ψ_0 is small enough to approximate $R_L^L(\pi/2-\phi+\psi)$ by $R_L^L(\pi/2-\phi)$ throughout the interval (ψ_1,ψ_2) . To analyze the reflection, the inhomogeneous beam with amplitude $A(\psi)$ is simplified to an homogeneous beam of amplitude A_0 , where

$$A_0 = \frac{1}{\psi_2 - \psi_1} \int_{\phi_1}^{\phi_2} A(\psi) \, d\psi \,. \tag{32}$$

Thus A_0 is the average of $A(\psi)$ across the crack. As far as the reflection is concerned the incident beam is now a plane longitudinal wave of amplitude $R_L^L(\pi/2 - \phi)A_0$. In addition it is assumed that the scattering is in the high-frequency range, i.e.,

$$k_L d \gg 1$$
, (33)

and that we seek a solution in the farfield, i.e.,

$$d/r \ll 1. \tag{34}$$

With these three assumptions we can use UAT as described in the previous section.

Let the point on the transducer be at x+y in the coordinate system on II as defined in Fig. 4. Here x is the coordinate of the transducer center, and y specifies the point on the transducer. Since the transducer length is 2l, we have $-l \le y \le l$.

We now make a final assumption, which is not essential to the analysis, but which helps simplify the expressions for the diffraction angles θ_j (j=1,2) of Fig.

4. The assumption is that

$$(x/d), (l/d) = O(1),$$
 (35)

which implies that all observations are made near the boundary of the reflection zone. With this assumption, we have

$$\theta_1 = 2\pi - \phi + [(x + y + d\sin\phi)/r][1 + O(d/r)],$$
 (36)

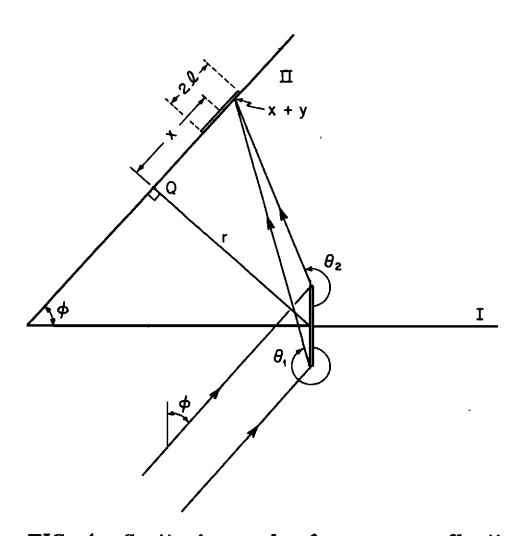


FIG. 4. Scattering angles for corner reflection.

$$\theta_2 = \pi + \phi - [(x+y-d\sin\phi)/r][1+O(d/r)],$$
 (37)

thus the delay factors t_j , s_{Lj} , j=1,2 of Eqs. (11) and (12) become

$$t_1 = (2k_L r)^{1/2} \sin \phi [1 + O(d/r)], \qquad (38)$$

$$t_2 = t_1 [1 + O(d/r)],$$
 (39)

and

$$s_{L1} = (\frac{1}{2}k_L r)^{1/2} [(x+y+d\sin\phi)/r] [1+O(d/r)], \qquad (40)$$

$$s_{L2} = -(\frac{1}{2}k_L r)^{1/2} [(x+y-d\sin\phi)/r] [1+O(d/r)].$$
 (41)

Hence,

$$t_1, t_2 \gg 1 \,, \tag{42}$$

and we may use the asymptotic form of F(z) from (28) to obtain

$$F(t_1) + F(t_2) - H(-x_2) = 1 + O[(k_L r)^{-3/2}].$$
 (43)

In the total field according to UAT from Eq. (25), the diffracted field \mathbf{u}_L^L is canceled by the singular part of $F(s_{L1}) + F(s_{L2})$, to leave

$$\mathbf{u}^{t} - \mathbf{u}^{i} = R_{L}^{L} \left(\frac{\pi}{2} - \phi \right) A_{0} \frac{e^{-i \, \tau_{4}}}{\pi^{1/2}}$$

$$\times \sum_{j=1,2} \left(\int_0^{s_{Lj}} e^{it^2} dt + \frac{i}{2s_{Lj}} (e^{is_{Lj}^2} - 1) \right) \mathbf{u}^L , \qquad (44)$$

where \mathbf{u}^L is the reflected L wave of Eq. (7). We may use the expressions for s_{L_i} of Eqs. (40) and (41),

$$\int_{0}^{s_{L1}} e^{it^{2}} dt + \int_{0}^{s_{L2}} e^{it^{2}} dt = \int_{t_{0}-t_{1}}^{t_{0}+t_{1}} e^{it^{2}} d\xi, \qquad (45)$$

where.

$$\xi_0 = (\frac{1}{2}k_L r)^{1/2} [(x+y)/r], \qquad (46)$$

$$\xi_1 = (\frac{1}{2}k_L r)^{1/2} (d/r) \sin \phi. \tag{47}$$

Therefore,

$$\mathbf{u}^{t} - \mathbf{u}^{i} = \hat{\mathbf{r}} A_{0} R_{L}^{L}(\phi) R_{L}^{L}(\pi/2 - \phi) \frac{e^{ik_{L}r}}{\pi^{1/2}}$$

$$\times \left(\int_{\xi_{0}^{-\xi_{1}}}^{\xi_{0}^{+\xi_{1}}} e^{i \cdot (\xi^{2} - \tau/4)} d\xi + \frac{e^{i \cdot \tau/4}}{\xi_{1}^{2} - \xi_{0}^{2}} \right)$$

$$\times \left\{ e^{i \cdot (\xi_{0}^{2} + \xi_{1}^{2})} \left[\xi_{1} \cos(2\xi_{0}\xi_{1}) - i\xi_{0} \sin(2\xi_{0}\xi_{1}) \right] - \xi_{1} \right\} ,$$

$$(48)$$

where $\hat{\mathbf{r}}$ is the unit vector in the direction of the transducer. This expression gives the corner reflection at any point on the transducer.

IV. TRANSDUCER

In the preceding two-dimensional analysis the dimensions and the properties of the transducer have not entered explicitly. The modeling of the transducer is briefly considered in this section.

The transducer is in contact with the free surface I, as shown in Fig. 1. It is assumed that the contact surface is a circle of radius l, which transmits a beam of essentially longitudinal waves. The signal may not be

uniform across the beam, but it is axially symmetric about a central ray. The beam may be convergent (focused) or divergent (as considered in this paper). The transmission properties of the transducer are defined by a function $f(\rho)$, where ρ is the radial distance from the center, with the normalization

$$\frac{2}{l^2} \int_0^1 f(\rho) \rho \, d\rho = 1 \,. \tag{49}$$

The transducer diameter 2l is small as compared to the crack width and as compared to the distance between the transducer and the crack. For the present geometry, which is shown in Fig. 1, it is then justifiable to consider the scattering as confined to planes normal to the crack edge, i.e., normal to planes I and II. Let III denote the plane through the center of the transducer normal to the crack edge. There will be scattering under angles with plane III, but its effect on the back-scattered field measured over the width 2l of the transducer will be small, and it will not change much as the transducer is moved along II. Since 2l is of the same order of magnitude as the crack depth d, we must, however, maintain the length dimension 2l in the plane II.

In view of these observations we will integrate the transducer properties in the direction normal to III, but maintain its length dimensions in the intersection of II and III. In this manner the transducer is modeled in a two-dimensional geometry as a line element of length 2l, as shown in Fig. 1.

The beam generated by the line element has a radius of curvature γ_0 , and it subtends an angle of $2\psi_0$, where

$$l = r_0 \tan \psi_0. \tag{50}$$

The displacement amplitude is not uniform across the beam, but it is symmetric about the central ray. Let the angle $\psi\epsilon(-\psi_0,\psi_0)$ denote a single ray, then the cross-sectional width of the circular transducer at the point on the line model where the ray defined by ψ crosses is $2l(1-\tan^2\psi/\tan^2\psi_0)^{1/2}$. By virtue of the integration of the transducer in the direction normal to plane III, the amplitude $A(\psi)$ corresponding to the line model is

$$A(\psi) = 2C_1 l \left(1 - \frac{\tan^2 \psi}{\tan^2 \psi_0} \right)^{1/2} \int_0^1 f[\rho(t)] dt , \qquad (51)$$

where the function f(r) defined by (49) has been used and

$$\rho(t) = l \left(t^2 + (1 - t^2) \frac{\tan^2 \psi}{\tan^2 \psi_0} \right)^{1/2} . \tag{52}$$

In Eq. (51) C_1 is a constant which depends on the transducer and its coupling to the free surface.

When the transducer acts as a measuring device, we assume that the line model receives in the same way that it emits, except that the characteristic function is taken as $g(\rho)$. Thus if $u(\psi)$ is the displacement from a normally incident wave at the point on the line model crossed by the ray, then the displacement as measured by the whole transducer is U.

$$U = \frac{r_0}{\pi l^2} \int_{-\phi_0}^{\phi_0} u(\psi) B(\psi) \sec^2 \psi \, d\psi \,, \tag{53}$$

169

J. Acoust. Soc. Am., Vol. 70, No. 1, July 1981

J. D. Achenbach and A. N. Norris: Diffracted signals for a crack

where

$$B(\psi) = 2C_2 l \left(1 - \frac{\tan^2 \psi}{\tan^2 \psi_0} \right)^{1/2} \int_0^1 g[\rho(t)] dt .$$
 (54)

Here C_2 is another transducer constant and $\rho(t)$ is defined by Eq. (52). For example, if $u(\theta) = u_0$, a constant, then $U = C_2 u_0$.

For our purposes we shall take the characteristic functions to be constants, therefore

$$f(\rho) = g(\rho) = 1 \tag{55}$$

$$A(\psi) = 2C_1(l^2 - r_0^2 \tan^2 \psi)^{1/2}, \qquad (56)$$

$$B(\psi) = 2C_2(l^2 - r_0^2 \tan^2 \psi)^{1/2}. \tag{57}$$

V. INTERFERENCE OF CORNER REFLECTION AND EDGE DIFFRACTION

We have already examined the corner reflection. Below, we shall derive the field on the transducer due to the edge diffraction. Then we will sum the two distinct effects and use the transducer model of the previous section to determine the response as a function of frequency and transducer position.

The edge-diffracted rays have the shortest travel time. The angles of incidence and diffraction are approximately ϕ and $\pi + \phi$, see Fig. 1. Thus the diffraction coefficient is approximately $D_L^L(\pi + \phi; \phi)$, where $D_L^L(\theta; \theta_L)$ is defined by Eq. (18). The ray which strikes the crack tip is defined by the angle ψ^- , given by Eq. (31). If $|\psi^-| > \psi_0$, then no ray strikes the crack tip and no edge diffraction is observed, although corner reflection may be observed. However, if there is edge diffraction then there will also be corner reflection. Assuming that $|\psi^-| < \psi_0$, then the diffracted field in the neighborhood of the transducer is \mathbf{u}^d , where

$$\mathbf{u}^{d} = \hat{\mathbf{r}} A(\psi^{-}) (k_{L} \gamma)^{-1/2} D_{L}^{L} (\pi + \phi; \phi) e^{i k_{L} (\gamma - 2d \cos \phi)}. \tag{58}$$

The phase due to the path length traveled has been calculated by using the assumption of Eq. (34) that $d/r \ll 1$.

The total displacement amplitude at the point y on the transducer due to corner-reflected rays and edge-dif-

fracted rays follows from Eqs. (48) and (58) as u(y):

$$u(y) = [A(\psi^{-})(k_L r)^{-1/2} D_L^L(\pi + \phi; \phi) e^{-2ik_L d \cos \phi} + \pi^{-1/2} A_0 R_L^L(\phi) R_L^L(\pi/2 - \phi) G(y)] e^{ik_L r},$$
(59)

where

$$G(y) = \int_{\xi_0 - \xi_1}^{\xi_0 + \xi_1} e^{i \cdot (\xi^2 - \pi/4)} d\xi + \frac{e^{i \cdot \pi/4}}{\xi_1^2 - \xi_0^2} \{ [\xi_1 \cos(2\xi_0 \xi_1) - i\xi_0 \sin(2\xi_0 \xi_1)] e^{i \cdot (\xi_0^2 + \xi_1^2)} - \xi_1 \},$$
(60)

and ξ_0 , ξ_1 are given by Eqs. (46) and (47). It is noted that u(y) is the superposition of two waves whose phase difference depends on d.

We assume a constant characteristic function, so that $A(\psi^{\gamma})$ is given by Eq. (56). The amplitude A_0 then follows from Eq. (31) as

$$A_0 = \frac{2C_1}{(\psi_2 - \psi_1)} \int_{\phi_1}^{\phi_2} (l^2 - r_0^2 \tan^2 \psi)^{1/2} d\psi.$$
 (61)

In Eq. (59) we now use the substitution

$$y = -r_0 \tan \psi \,, \tag{62}$$

and we substitute the result in Eq. (53), to obtain

$$U = C_2 [A(\psi^{-})(k_L r)^{-1/2} D_L^L(\pi + \phi; \phi) e^{-2ik_L d \cos \phi}$$

$$+ 2\pi^{-3/2} l^{-2} A_0 R_L^L(\phi) R_L^L(\pi/2 - \phi)$$

$$\times \int_{-1}^{1} (l^2 - y^2)^{1/2} G(y) dy] e^{ik_L r} .$$
(63)

It is noted that U/C_1C_2 is a function of the seven parameters k_L , r, ϕ , d, x, l, and r_0 .

VI. RESULTS AND DISCUSSION

For $\phi=\pi/4$, d=1, r=20, and l=0.5 the dimensionless transducer response \overline{U} , where $\overline{U}=U/C_1C_2$ and U is given by Eq. (63), has been plotted versus the dimensionless frequency $\omega d/c_L$, for several values of x and two values of r_0 . In the computations $c_L/c_T=2$, which corresponds approximately to aluminum or titanium

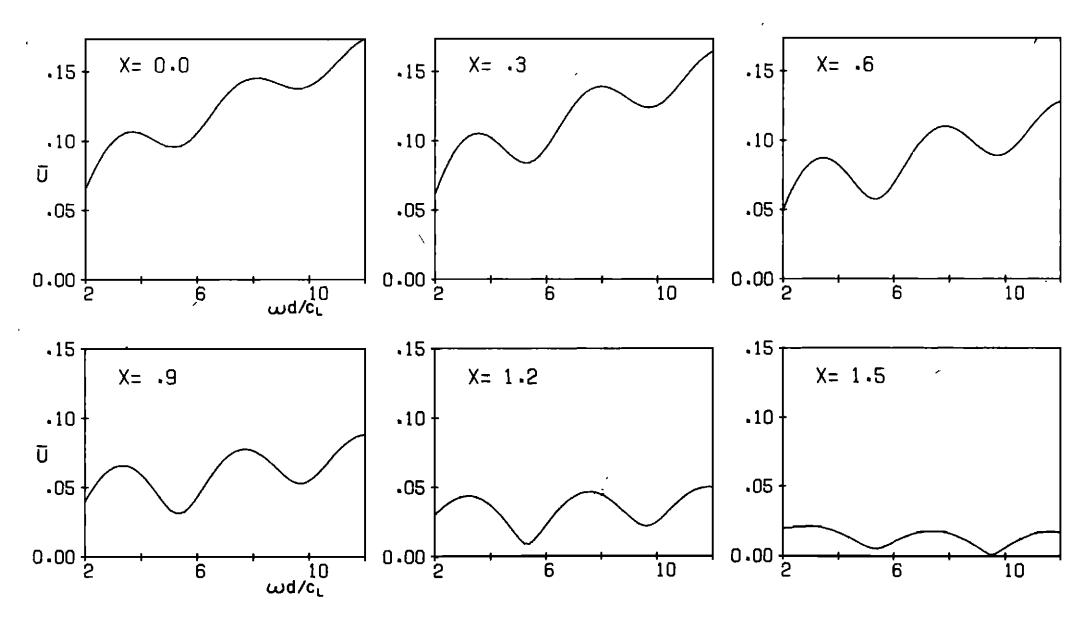


FIG. 5. Amplitude versus frequency curves for various positions of the transducer, for $r_0=20$.

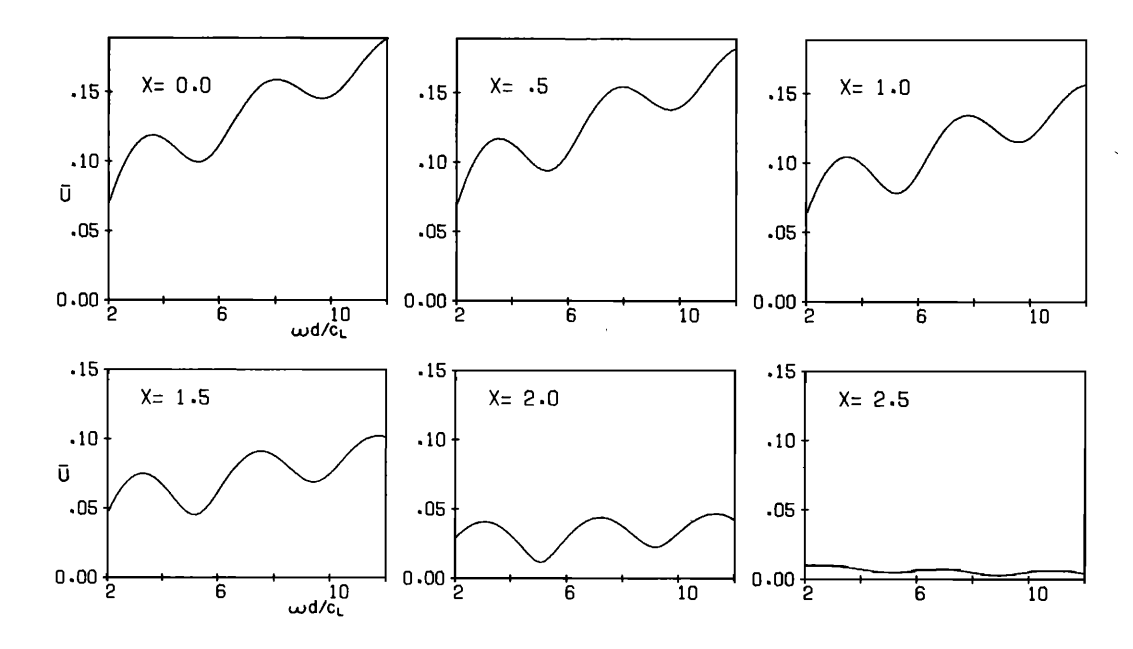


FIG. 6. Amplitude versus frequency curves for various positions of the transducer, for $r_0 = 7$,

In Fig. 5, $r_0 = 20$ and x varies from 0 to 1.5 in increments of 0.3. In Fig. 6, $r_0 = 7$ and x varies from 0 to 2.5 in increments of 0.5. The trend is similar in both cases. For small x, the response increases with the frequency. This is to be expected since at x = 0 the transducer is in the region of maximum corner reflection. The edge diffraction is also present, but it produces oscillations which are small relative to the total amplitude. As x is increased, the contribution of the corner reflection decreases faster than that of the edge diffraction. Just before a cutoff distance is reached at which the corner reflection virtually vanishes, the two effects are of approximately equal magnitude, giving a good interference pattern in which the "peak to valley" ratio is large. For this position of the transducer the interference pattern would probably be best recognizable from experimental data. However, the region in which this effect is present is confined to a small zone just before the cutoff distance. If the transducer is moved slightly away from this zone, then the distinct interference disappears.

It is noted that the period of oscillation correlates with the simple interference equation

$$(\omega d/c_L)\cos\phi = \pi \,, \tag{64}$$

for which, $\omega d/c_L \approx 4.44$ in our example. Thus measurement of the period leads to an estimation of the crack depth.

Finally, the fact that the cutoff distance is larger for $r_0 = 7$ than it is for $r_0 = 20$ is attributable to the wider spreading of the beam in the former case; thus the transducer may be moved over a greater range while still permitting a significant part of the beam to interact with the crack.

ACKNOWLEDGMENT

This work was carried out in the course of research sponsored by the Center for Advanced NDE operated by the Science Center, Rockwell International for the Advanced Research Project Agency and the Air Force Materials Laboratory under Contract F33615-80-C-5004.

¹P. A. Doyle and C. M. Scala, "Crack Depth Measurement by Ultrasonics: A Review," Ultrasonics 16, 164-171 (1978).

⁴R. M. Lewis and J. Boersma, "Uniform Asymptotic Theory of Edge Diffraction," J. Math. Phys. 10, 2291-2305 (1969).

²S. Golan, L. Adler, K. V. Cook, R. K. Nanstad, and T. K. Bolland, "Ultrasonic Diffraction Technique for Characterization of Fatigue Cracks," J. Nondestructive Eval. 1, 11-20 (1980).

³J. D. Achenbach, A. K. Gautesen, and H. McMaken, "Application of Elastodynamic Ray Theory to Diffraction by Cracks," in *Modern Problems in Elastic Wave Propagation* (Wiley-Interscience, New York, 1978).

⁵S. W. Lee, "Uniform Asymptotic Theory of Electromagnetic Edge Diffraction: a Review," Electromagnet. Lab. Rep. 77 77-1 (University of Illinois at Urbana-Champaign, 1977).